

2024

Optimization of High-Bypass Turbofan High-Pressure Compressor Blade – A Case Study

Adeel Khalid

Kennesaw State University, akhalid2@kennesaw.edu

Vlad Mandzyuk

Kennesaw State University, mandzyukvlad@gmail.com

Follow this and additional works at: <https://digitalcommons.kennesaw.edu/kjur>



Part of the [Aerodynamics and Fluid Mechanics Commons](#), [Computer-Aided Engineering and Design Commons](#), and the [Propulsion and Power Commons](#)

Recommended Citation

Khalid, Adeel and Mandzyuk, Vlad (2024) "Optimization of High-Bypass Turbofan High-Pressure Compressor Blade – A Case Study," *The Kennesaw Journal of Undergraduate Research*: Vol. 11: Iss. 1, Article 4.

DOI: <https://doi.org/10.62915/2474-4921.1250>

Available at: <https://digitalcommons.kennesaw.edu/kjur/vol11/iss1/4>

This Article is brought to you for free and open access by the Active Journals at DigitalCommons@Kennesaw State University. It has been accepted for inclusion in The Kennesaw Journal of Undergraduate Research by an authorized editor of DigitalCommons@Kennesaw State University. For more information, please contact digitalcommons@kennesaw.edu.

OPTIMIZATION OF HIGH-BYPASS TURBOFAN HIGH-PRESSURE COMPRESSOR BLADES – A CASE STUDY

Vlad Mandzyuk

*Kennesaw State University
Marietta, GA, United States*

Dr. Adeel Khalid

*Kennesaw State University
Marietta, GA, United States*

ABSTRACT

This research determines the relationship between the High-Pressure Compressor (HPC) rotor blade design variables and compressor pressure ratio of a high bypass turbofan engine. Alterations in the HPC blades span, chord, taper, twist, number, and angle of incidence are performed and their effect on the HPC pressure ratio is observed. The objective is to determine key parameters that could maximize the performance of a high-pressure compressor for a given mission. Physics-based modeling, Computational Fluid Dynamics (CFD), and wind-tunnel testing are performed to compare and validate findings. Physics-based modeling is performed to serve as the benchmark for data obtained through other methods. CFD analysis replicates wind-tunnel testing within a computer setting. In this experiment, the first stage of the high-pressure compressor is designed and simulated. Upon the completion of these experiments, wind-tunnel testing is conducted to validate results. Data is compared in the form of graphs relating the stage pressure ratio of the HPC to the corresponding blade design variable. The objective of this study is to optimize the design of the HPC using the discovered design variables related to the maximum pressure ratios to maximize the engine performance. This will result in lower operating costs, longer range, and lower emissions. When implemented, the engine optimized for the specific mission could save the aircraft manufacturer and operators the initial and operating expenses. Additionally, solutions to the following questions are explored. Do the use of CAD (Computer Aided Design) and CFD models provide a feasible solution for gas turbine engine optimization? Do the results obtained from CFD analyses show the same level of improvement in engine performance as obtained by physics-based models? This study is a comparative analysis between the different blade design variables and will compare the level of accuracy between each experiment.

KEY WORDS

Gas turbine engine, CFD, physics-based modeling, wind-tunnel, high-pressure compressor

NOMENCLATURE

a_0 – speed of sound

a_{std} – speed of sound on a standard day

b – span

β – angle of incidence

c - chord

N – number of stages

P_t – total pressure

P_{tN} -total pressure at stage N

S_{pj} – compressor blade area

π_c – compressor pressure ratio

π_s – stage pressure ratio

I. BACKGROUND AND INTRODUCTION

The compressor pressure ratio is a valuable parameter to consider when studying gas turbine engines. The pressure ratio is the ratio of the pressure at the outlet of the compressor to the inlet of the compressor. The objective of the compressor is to pressurize as much air as possible prior to the air entering the combustion chamber. This will elevate the performance of the combustion chamber and improve the engine's overall efficiency. Previous methods to improve the compressor pressure ratio included increasing the number of stages within a compressor. This design process improves the engine's pressure ratio but adds weight the more stages are added to the point where the pressure ratio eventually does not increase. This research focuses on determining the effect of modifying the high-pressure compressor (HPC) blades on the engine's compressor pressure ratio. This is explored to determine if it is feasible to improve the compressor pressure ratio without significantly adding weight to the engine.

The results of this study are used to compare and determine the optimal blade design

variables of the HPC to improve the performance of the turbofan engine. Three methods are used to perform this study: Physics-based modeling, CFD analysis, and wind-tunnel testing. Physics-based modeling is a mathematical approach to relating the compressor pressure ratio and the design variable of the blades. This method will serve as the benchmark for data gathered through CFD and wind-tunnel testing. CFD analysis is performed using SolidWorks software that can simulate the air flowing through the compressor, giving us results for the compressor pressure ratio. Wind-tunnel testing is conducted to gather experimental data. Wind-tunnel tests will be used to validate the results obtained from CFD analysis.

The blades of study are based on the first stage of the HPC of the GENx-1B turbofan engine. The span, chord, angle of incidence, taper, twist, and number of blades in each compressor stage will be altered to observe how the pressure ratio is changed. Table 1 indicates the baseline values and the design variations made to the HCP blade.

Table 1. The design table details the modifications made to the baseline blade

Deviation from Baseline Blade	Blade Design Variable					
	Span Length	Average Chord Length	Angle of Incidence	Twist	Taper Ratio	Number of Blades
-10%	0.1756 m	0.1638 m	44.64°	-10 °	-1	30
-5%	0.1853 m	0.1731 m	47.12 °	-5 °	-0.5	31
0%	0.1951 m	0.1821 m	49.6 °	0 °	0	33
5%	0.2048 m	0.1912 m	52.08 °	5 °	0.5	35
10%	0.2146 m	0.2003 m	54.56 °	10 °	1	36

These values are used to create the models used in all experimental methods. It is important to mention that even though the values are based on an existing engine, they are the best engineering

estimates of the existing design. This does not affect the study because it is a comparative analysis. Figure 1 displays the model of the first stage of the high-pressure compressor created in SolidWorks. This model will be the basis for

physics-based modeling to gather information on the projected area, CFD analysis, and for 3D printing prototypes for wind-tunnel testing. The SolidWorks model used was recreated using an existing model created by Klisz [1]. The model obtained was found to be the most accurate and complete CAD model of the GENx-1B turbofan engine. Figure 1 shows the recreated model from SolidWorks used in the analysis.

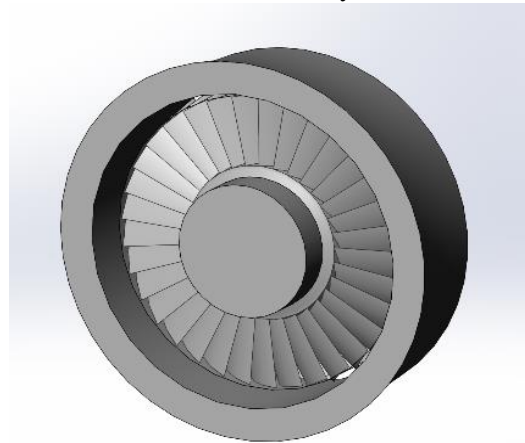


Figure 1. SolidWorks CAD model of 1st stage high-pressure compressor [1]

The flight variables will be based on cruising conditions for the GENx-1B. The aircraft this engine is designed for, the B787-Dreamliner, has a cruise Mach of 0.85 and a cruise service ceiling of 13,106 m. [2]. All calculations conducted are under the assumption of cruising conditions on a standard day.

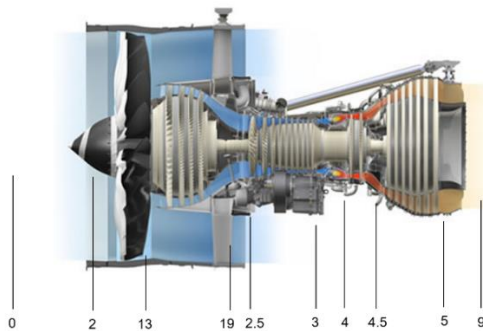


Figure 2. GENx-1B station numbering [3]

Due to the inconsistent station numbering conventions for many publications, this research

focuses on the one presented in Figure 2. This convention is based on the one provided by Mattingly [3].

II. PHYSICS-BASED MODELING

This method is a mathematical approach to relating the blade design variables to the compressor pressure ratio. Utilizing the lift equation, a ratio of the blade lift with an adjusted design variable to the baseline blade lift is related to the theoretical stage pressure ratio. The stage pressure ratio is the ratio of the pressure leaving the stage to the pressure entering the stage. The stage pressure ratio is related to the compressor pressure ratio by the following equation:

$$1. \quad \pi_c = \pi_s^N$$

Since this study focuses on only the first stage of the HPC, stage pressure ratio will be the variable studied. The lift equation is given by:

$$2. \quad L = \frac{1}{2}\rho V^2 C_l S_{pj}$$

L represents the lift generated by the first stage of the HPC. ρ represents the density at the cruise service ceiling. V represents the velocity of the fluid flowing through the compressor. C_l is the coefficient of lift and S_{pj} is the projected area of the blade multiplied by the number of blades within a stage. The lift ratio and pressure ratio will be related by the following equation:

$$3. \quad \frac{L}{L_{BL}} = \frac{\pi_s}{\pi_{sBL}}$$

Table 2. Initial Parameters used in Physics-Based Modeling

Preliminary Flight and Engine Parameters [4]			
Density	Velocity	Stage Pressure Ratio	Compressor Pressure Ratio
0.2776 kg/m ³	121.92 m/s	1.28	11.81

The blade shown in Figure 3 is altered according to the blade design variables from

Table 1. The figure is useful in determining the resulting projected area of the blade. The projected area is multiplied by the total number of blades at a given stage to effectively compare each blade design variable to the number of blades parameter. In the lift equation, the velocity and density remain constant for all deviations. The coefficient of lift is the same for all parameters except for the angle of incidence. The coefficient of lift is directly related to the angle of attack, so linear interpolation is performed to obtain the proper coefficient of lift for the blade design variable. The other parameter that affects the coefficient of lift is twist. The coefficient of lift in the lift calculations remains constant for the twist blade design variable because the impact on the coefficient of lift from the changes in twist is insignificant. The ideal way to calculate the coefficient of lift is to do blade element analysis. Since the changes in twist are small, they have little impact on the coefficient of lift and as such the lift ratio.

Additional assumptions are that this is an isentropic compression and expansion process, the working fluid (air) behaves as a perfect gas with constant specific heats, and there is no bleed or cooling flows. These assumptions lead physics-based modeling to overpredict real values for stage pressure ratio when compared to wind-tunnel testing. The objective is to perform a comparative analysis and find what trends occur when modifying blade design variables.

The method of converting the calculated lift to the stage pressure ratio is done by obtaining lift ratios. The lift ratio in this study is the calculated lift at a design variable at a certain deviation from the baseline blade over the lift of the baseline blade. Based on this method, the baseline lift is determined to be 1039.23 N and is the same for every design variable used to calculate lift ratio. The lift ratio is then multiplied by the baseline stage pressure ratio [4] to obtain the stage pressure ratio at a specific design parameter. This is shown in equation 3. The stage pressure ratio is the air leaving the first rotor stage

of the HPC over the air entering the first rotor stage HPC. Table 3 shows the results gathered from physics-based modeling.

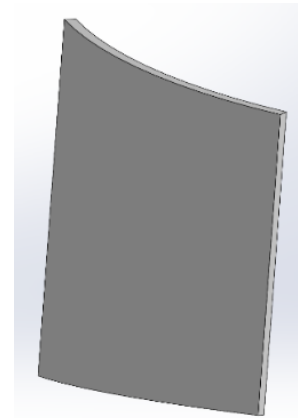


Figure 3. An example of the HPC blade created in SolidWorks

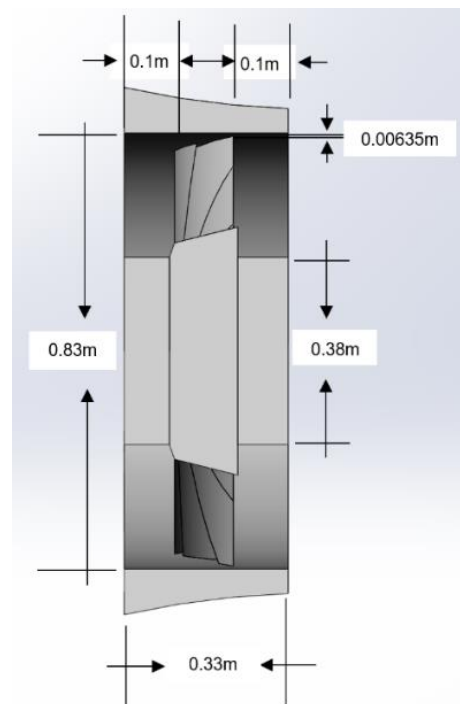


Figure 4. Dimensions of the first stage of the high-pressure compressor

Table 3. Physics-based modeling results

Blade Design Variable	Deviation from Baseline Blade	Lift and Pressure Ratio			
		Lift	Lift Ratio (Lift / Baseline Lift)	Stage Pressure Ratio	Compressor Pressure Ratio
Baseline	0%	1039.23 N	1.0	1.28	11.81
Span	-10%	926.55 N	0.89	1.14	3.75
	-5%	980.80 N	0.94	1.21	6.62
	5%	1093.49 N	1.05	1.35	19.64
	10%	1151.92 N	1.11	1.42	33.05
Chord	-10%	943.24 N	0.91	1.16	4.48
	-5%	989.15 N	0.95	1.22	7.20
	5%	1085.14 N	1.04	1.34	18.19
	10%	1135.23 N	1.09	1.40	28.56
Angle of Incidence	-10%	868.17 N	0.84	1.07	1.95
	-5%	951.02 N	0.92	1.17	4.86
	5%	1126.87 N	1.08	1.39	26.53
	10%	1216.07 N	1.17	1.50	56.83
Twist	-10%	1043.41 N	1.00	1.29	12.29
	-5%	1043.41 N	1.00	1.29	12.29
	5%	1039.23 N	1.00	1.28	11.81
	10%	1035.06 N	1.00	1.27	11.34
Taper	-10%	997.50 N	0.96	1.23	7.84
	-5%	1018.37 N	0.98	1.25	9.64
	5%	1064.28 N	1.02	1.31	14.98
	10%	1085.14 N	1.04	1.34	18.19
Number of Blades	-10%	944.76 N	0.91	1.16	4.55
	-5%	976.25 N	0.94	1.20	6.32
	5%	1102.22 N	1.06	1.36	21.26
	10%	1133.71 N	1.09	1.40	28.18
Optimized	---	1532.10 N	1.47	1.89	572.61

After the physics-based analysis is completed, four design variables show the greatest impact on the increase of the compressor pressure ratio: span length, chord length, angle of incidence, and number of blades. These design variables show the highest increase at +10% deviation from the baseline blade. These blade design variables show an increasing trend of the compressor pressure ratio as the deviation from the baseline increases. The taper ratio displays a smaller rate of increase while the deviation in twist shows a decrease in the compressor pressure ratio. The twist has its highest-pressure ratio at -10% deviation from the baseline blade. The stage pressure ratio is highest at +10% deviation for the

taper ratio parameter. This method is performed to determine which variables increase the compressor pressure ratio the greatest. The optimized model has a 38.49% higher stage pressure ratio than the baseline model. The results of this method are graphed in Figures 12-17. The optimized model is the combination of all the design variables in which they had the greatest stage pressure ratio. This is span, chord, angle of incidence, number of blades, and taper at +10% and twist at -10% deviation from the baseline blade.

Table 4 displays the physics-based modeling results for the baseline and optimized high-pressure compressor models at increasing

speeds. This analysis is performed to compare the trends obtained in this method with the results of the wind-tunnel testing. As the percent max speed of the wind-tunnel increases, the stage pressure ratio also increases. The optimized model portrays higher stage pressure ratio values than the baseline model as expected. The optimized model is the combination of the design variables at the percent deviation from the baseline blade that produces the highest stage pressure ratio. This can be observed in Table 3. The maximum speed used in this study is 145 MPH (64.82 m/s) to effectively compare with data obtained from wind-tunnel testing.

Table 4. Physics-based modeling results for baseline and optimized HPC models at increasing speeds

Percentage of Maximum Speed	Baseline π_s	Optimized π_s
5 %	0.05	0.08
10%	0.20	0.30
15%	0.46	0.68
20%	0.82	1.21
25%	1.28	1.89
30%	1.84	2.72
35%	2.51	3.70
40%	3.28	4.83
45%	4.15	6.11
50%	5.12	7.55

At 50% of the max speed of the wind-tunnel, the optimized stage pressure ratio has a 38.36% higher stage pressure ratio than the baseline model. This means that combining the optimized design variables together still has a significant increase in the pressure ratio.

III. CFD ANALYSIS

This method is used to simulate the air flow through the compressor. The overall objective of this method is to determine if CFD analysis provides a good alternative to determining engine performance. This is done by observing the effect of altering the blade design variables on the stage

and compressor pressure ratio. Figure 4 shows the dimensions of the first stage of the HPC.

Unlike the physics-based modeling, this model contains a spool and an annulus. The experiment parameters are kept the same as the physics-based modeling as indicated in Table 2. Table 4 shows additional parameters that are needed to simulate this model. The parameters do not reflect the actual parameters of the GEnx-1B due to the limitations of CFD while attempting to run the simulations. This does not affect the overall objective of this research, which is to perform a normalized comparative analysis with set percentage changes from the baseline model. In addition, Figure 5 shows the setup of the simulation. For this study, the length of the compressor is 0.3327m. [1] The space between the front lid and front tip of the blade is the same for the rear lid of the compressor and rear tip of the blade. This space is 0.1016m. Another important dimension is the clearance. The clearance from the rear outer diameter of the blades to the inner diameter of the annulus is 0.0064m. These values are kept constant throughout the study and are representative of the base model.

The boundary conditions are from the inlet of the stage to the outlet. This is maintained through “lids,” which are shown in Figure 6. These lids are added to simulate an internal flow analysis. These lids are the boundary conditions for the inlet velocity and the environmental pressure.

Table 5: CFD analysis airflow parameters [5]

Airflow Parameters		
Inlet Velocity	Outlet Temperature	Outlet Pressure
121.92 m/s	74.15 °C	184.43 KPa

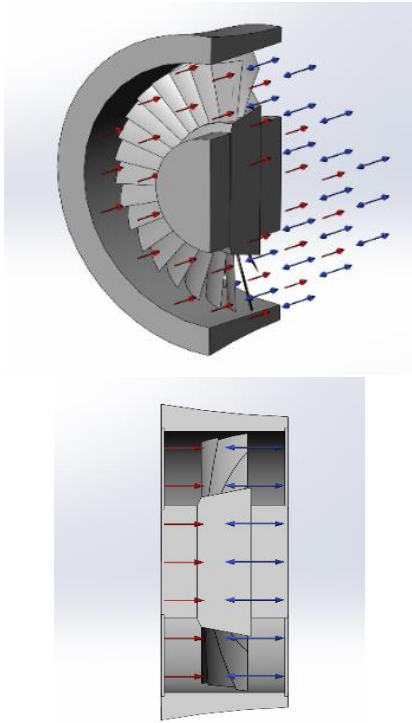


Figure 5. Flow simulation boundary conditions

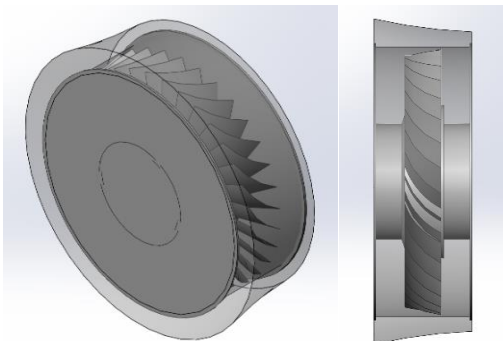


Figure 6. High-pressure compressor with lids

The inlet velocity is the velocity at station 2.5 (Figure 2). This velocity represents the air entering the high-pressure compressor. The outlet temperature and pressure are environmental parameters measured at station 3. These parameters are assumed to be the same as the outlet of the first stage of the high-pressure compressor. The velocity used is lower than the original 256.91 m/s due to SolidWorks flow simulation solver errors. The angular velocity of the HPC spool is 11,377 rpm (1192 rad/s) rotating

in a counterclockwise direction. [5] Figure 7 shows an example of a cut-plot retrieved from the CFD analysis. This cut-plot shows the pressure variation throughout the stage of the HPC.

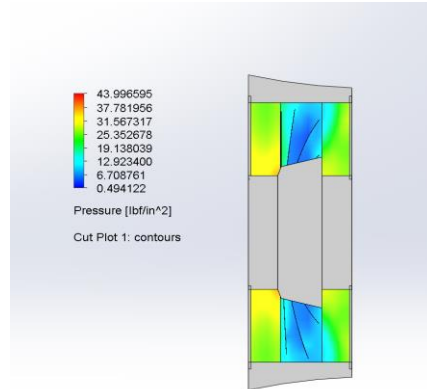


Figure 7. Example of pressure cut plot

The first simulation is of the baseline engine. The compressor characteristics are kept as the original high-pressure compressor. The blade characteristics are altered one at a time. Table 6 shows the results obtained.

Table 6. CFD analysis results

Blade Design Variable	Deviation from Baseline Blade	Pressure Ratio Results	
		Stage Pressure Ratio	Compressor Pressure Ratio
Baseline	0%	1.132	3.84
Span	-10%	0.98	1.30
	-5%	1.048	2.16
	5%	1.169	4.77
	10%	1.201	6.29
Chord	-10%	1.297	13.47
	-5%	1.208	6.87
	5%	1.101	3.7
	10%	1.015	1.16
Angle of Incidence	-10%	1.095	2.69
	-5%	1.125	3.27
	5%	1.234	8.19
	10%	1.286	12.37
Twist	-10%	1.504	59.05
	-5%	1.399	29.62
	5%	1.415	34.29
	10%	1.463	64.62

Taper	-10%	1.082	2.46
	-5%	1.097	2.53
	5%	1.19	9.93
	10%	1.428	35.21
Number of Blades	-10%	1.065	1.88
	-5%	1.078	2.12
	5%	1.193	5.86
	10%	1.287	12.47
Optimized	---	1.521	66.26

Two equations are used in the flow simulation to calculate the pressure ratio. π_s , the stage pressure ratio is calculated as the ratio of the pressure leaving the first stage of HPC to the pressure entering the first stage of HPC [1]. This ratio is obtained through flow simulation. The compressor pressure ratio π_c , determines the pressure ratio of the entire high-pressure compressor. This relation is shown in equation 1.

Once CFD analysis is completed, it is possible to observe the effect of blade design parameters on the compressor pressure ratio. The CFD analysis displayed similar trends as the physics-based modeling method for the span, angle of incidence, and number of blades in each stage parameters. The chord variable showed the opposite trend. When performing CFD, the stage pressure ratio decreased as the deviation in chord increased from the baseline blade. The twist parameter displayed an inconsistent trend. This could be due to a modeling error. The Taper ratio blade design variable showed an increasing trend like in the physics-based modeling, but at a greater rate of increase. Particularly from 5% to 10% deviation. These results are shown in Table 5 and compared with the results from the physics-based modeling in Figures 12-17.

IV. Wind-Tunnel Testing

The wind-tunnel tests are conducted using the wind-tunnel shown in Figure 8. The first stage of the HPC is 3D printed using ABS (Acrylonitrile butadiene styrene) material. Material type or surface roughness have no impact on the results of this comparative analysis. Models for a baseline and optimized version are

created. These models are tested using the wind-tunnel. Data for lift (axial force) is collected and used to compare the effect of the optimized stage to the compressor pressure ratio. The optimized models are those with blade design variables in which the highest-pressure ratio occurred.

The objective of performing wind-tunnel testing is to obtain real experimental data for how the pressure ratio changes with changing the blade design parameters. These results indicate the accuracy of the previous methods. The data is collected in increments of the percent of the maximum speed of the wind-tunnel. This is also another variable that can show how the pressure ratio can be increased or decreased. Since the models have been tested through physics-based modeling and through CFD, it is expected that the optimized models will generate a greater pressure ratio. Table 7 shows the data gathered through wind-tunnel testing. Unlike the physics-based modeling method, the optimized model did not lead to an improved stage pressure ratio. There was a 2.69% decrease from the baseline to the optimized models at 50% of the max wind-tunnel speed.



Figure 8. AEROLAB EWT wind-tunnel



Figure 9. An example of the output data provided by the AEROLAB EWT wind-tunnel

Table 7 displays the results of the wind-tunnel test. The first column represents the

percentage of maximum speed of the wind-tunnel. The data directly obtained from the wind-tunnel are the baseline axial force and optimized force columns. The axial force is converted to the stage pressure ratio to accurately compare the physics-based method to wind-tunnel testing. The axial force for the baseline and optimized models is divided by the baseline axial force at 25% max speed to convert them to non-dimensional values. This value is then multiplied by 1.28 (theoretical baseline stage pressure ratio [4]) to find the stage pressure ratio. Both models display an increasing trend of the stage pressure ratio as the percent max speed increased. The optimized model has slightly higher values of the pressure ratio than the baseline model.

Table 7. Wind-tunnel results

Percent of Maximum Speed	Model Type and Lift			
	Baseline Axial Force [N]	Baseline Stage Pressure Ratio	Optimized Axial Force [N]	Optimized Stage Pressure Ratio
5%	0.04	0.03	0.05	0.04
10%	0.27	0.19	0.28	0.20
15%	0.63	0.45	0.61	0.43
20%	1.12	0.79	1.11	0.78
25%	1.81	1.28	1.84	1.30
30%	2.62	1.85	2.58	1.82
35%	3.58	2.53	3.58	2.53
40%	4.71	3.33	4.65	3.29
45%	6.08	4.30	5.87	4.15
50%	7.47	5.28	7.27	5.14

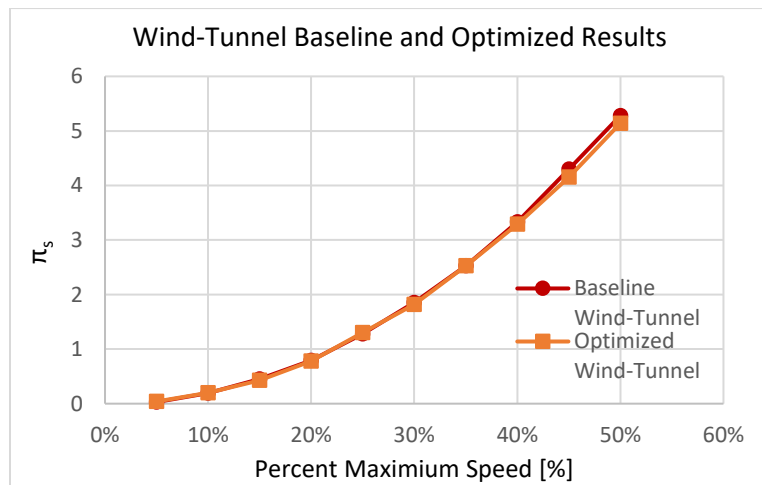


Figure 10. Wind-tunnel test results

The results shown in Table 7 are converted to lift and pressure ratios to effectively compare the results of the three methods conducted in this research. There are rotating models to try to replicate the CFD model since that model is also rotating. Figure 11 shows the 3D printed models. A baseline and an optimized model are 3D printed. The optimized model is the combination of the blade design variables in which the greatest stage pressure was calculated. This is also mentioned in the physics-based modeling method. Figure 12 shows how the model will be set up in the wind-tunnel.

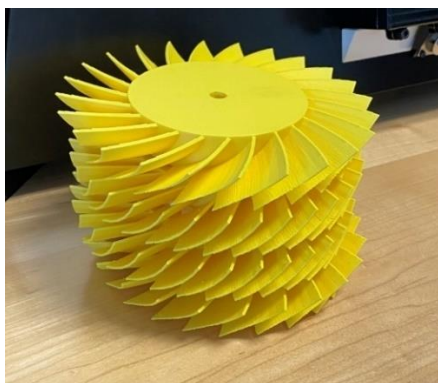


Figure 11. 3D printed models to be used in wind-tunnel testing



Figure 12. Wind-tunnel setup example

V. RESULTS AND DISCUSSION

The results of the physics-based modeling and CFD analysis are compared graphically. It can be seen from Figures 13-19 that the physics-based modeling tends to have higher values for stage pressure ratio than the CFD analysis. This can most likely be attributed to frictional losses that occurred in the CFD model. The increase in deviation of span from the baseline blade increased the stage pressure ratio for both models. It can be assumed and potentially confirmed with wind-tunnel testing that increasing the span can increase the stage pressure ratio of the high-pressure compressor. The optimized blade for the span blade design variable is at 10% deviation from the baseline blade for both methods. The physics-based modeling method showed a 10.73% increase in stage pressure ratio from the baseline value to the blade with a span of 10% deviation from the baseline. The CFD analysis has a 5.92% increase.

For the increase in deviation of chord from the baseline blade, the two methods yield conflicting trends. The stage pressure ratio increases as the deviation from the baseline blade in chord length is increased for physics-based modeling. The opposite is true for CFD analysis. This can be attributed to assumptions made in the physics calculations or an error in the simulations. The results should be confirmed through wind-tunnel testing. The optimal blade design for the chord parameter would be at 10% deviation from the baseline blade from the physics-based modeling. The optimal blade design from the CFD analysis would be at -10% deviation from the baseline blade. It is interesting to note that increasing the chord length decreases the pressure ratio in the CFD analysis. At 10% deviation from the baseline blade, the physics-based modeling method has a 10.73% increase in the stage pressure ratio. CFD analysis has a 13.59% increase in stage pressure ratio at -10% deviation from the baseline blade.

The angle of incidence, taper ratio, and number of blades blade design variables also display similar trends. That is, an increase in the stage pressure ratio occurs as the deviation from the baseline is increased in those design variables. The maximum stage pressure ratio occurs at +10%. These results are supported by both methods. The only difference in results is that physics-based modeling has higher stage pressure ratios than CFD analysis. At 10% deviation from the baseline blade, the stage pressure ratio increases by 15.83%, 4.58%, and 8.96% for the angle of incidence, taper, and number of blades design variables for the physics-based experiment respectively. For CFD analysis, the increase is 12.74%, 23.13%, and 12.82%.

The only blade design variable to have a negative impact on the stage pressure ratio is the twist variable. This is also supported by both methods, but the CFD analysis has more of an exponential curve and the physics-based modeling has a linear curve. The optimal deviation from the baseline blade occurred at -10% for both methods. At -10% of the deviation from the baseline blade, the stage pressure ratio increases by 0.78% and 11.33% for the physics based and CFD methods respectively. It can be concluded that twist has no significant impact on

the pressure ratio when performing physics-based modeling.

Considering the assumptions made, and the complete difference between both methods, the percent difference is relatively low. To further validate these results, wind-tunnel testing is conducted. Figure 10 shows the results of the wind-tunnel testing. Wind-tunnel testing is performed for a baseline model and an optimized model. The results of the method are compared with the results obtained from physics-based modeling. All four lines display the same trend of increasing stage pressure ratio as wind-tunnel speed is increased. The baseline models for both methods show very close values to each other confirming the accuracy of the calculations. CFD analysis for the same speeds presented solver errors and is not compared to these methods. The difference between all three methods can be attributed to frictional losses presented in wind-tunnel testing. In addition, there is a failure with the 3D printed models where they were not rotating as intended. This affected the study because rotation determines the amount of extraction of energy from the air. As a result, this is one of the possible reasons why the optimized model did not lead to an increase in stage pressure ratio.

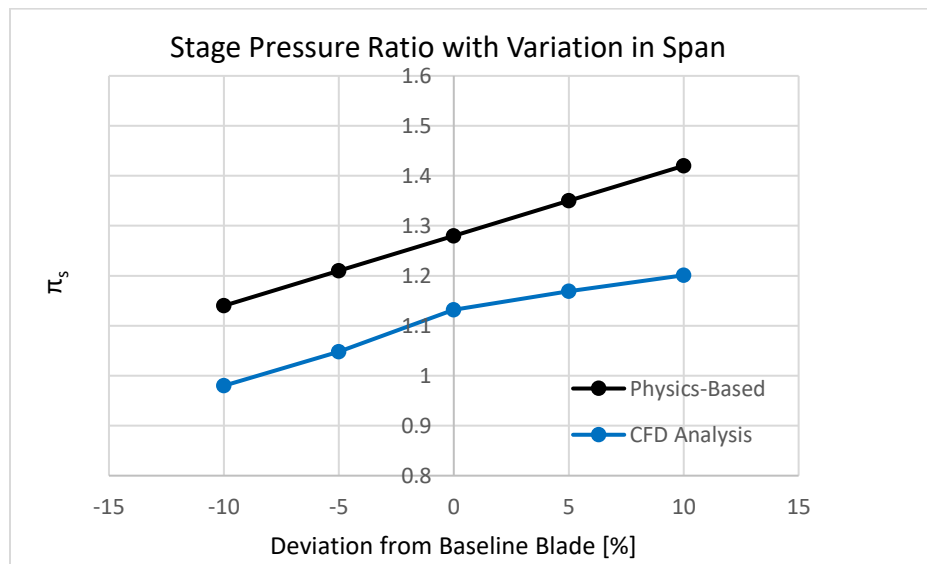


Figure 13. A plot of the stage pressure ratio with variations in span of the blade

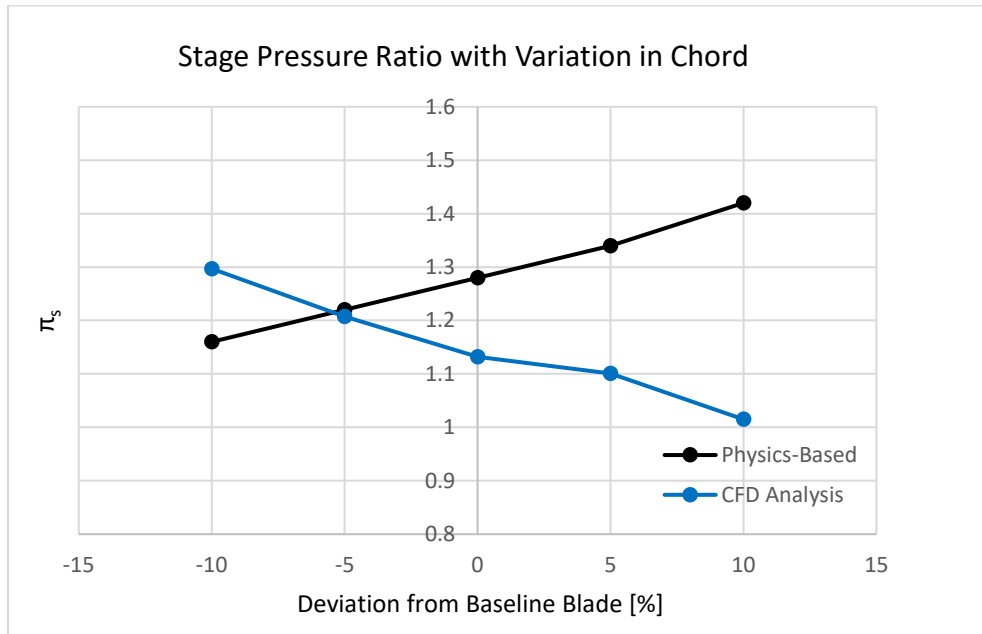


Figure 14. A plot of the stage pressure ratio with variations in chord of the blade

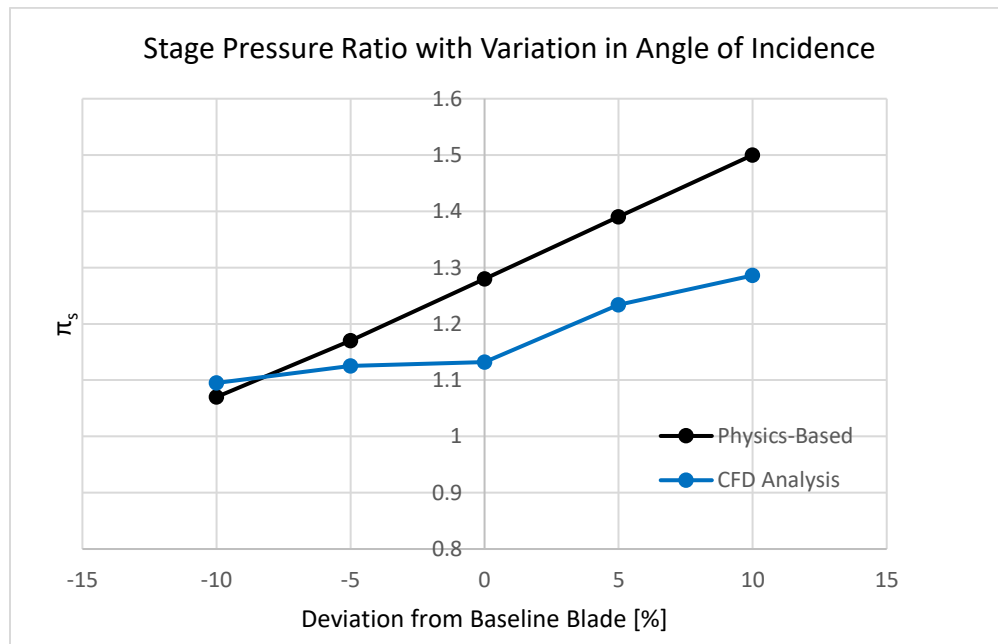


Figure 15. A plot of the stage pressure ratio with variations in angle of incidence of the blade

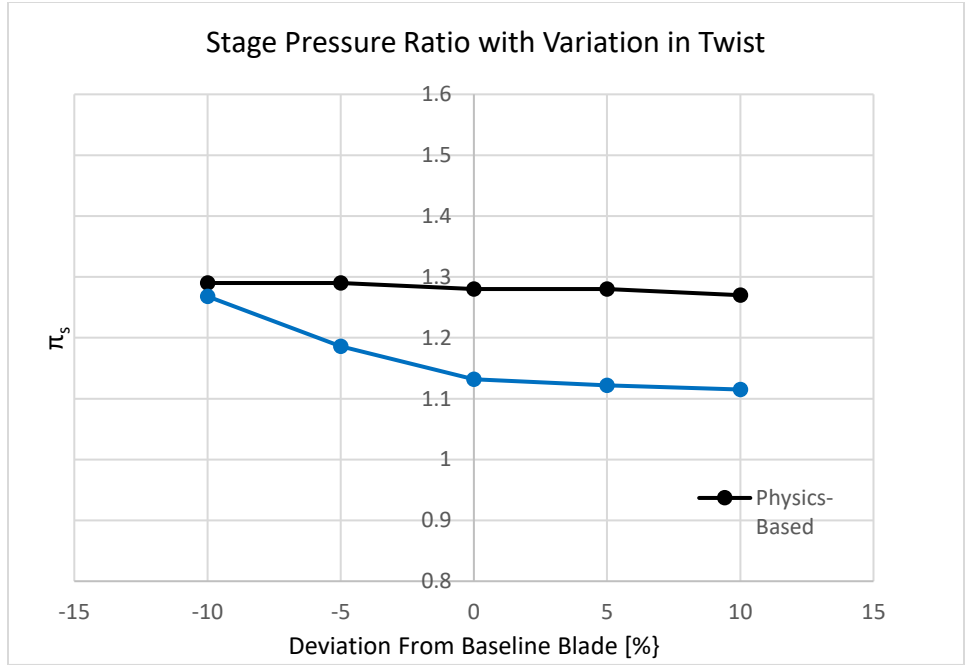


Figure 16. A plot of the stage pressure ratio with variations in twist of the blade

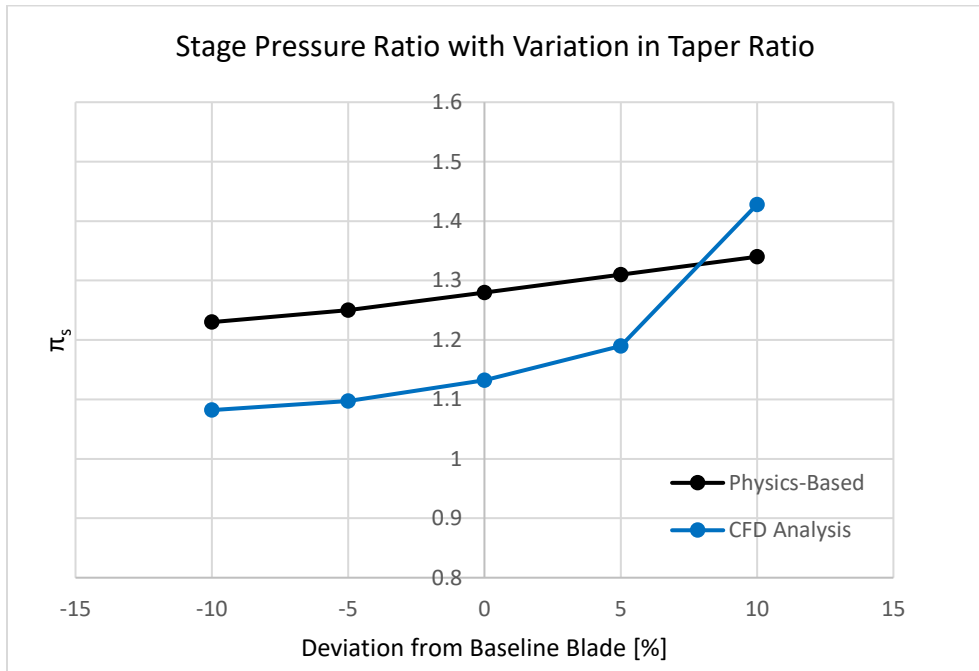


Figure 17. A plot of the stage pressure ratio with variations in taper ratio of the blade

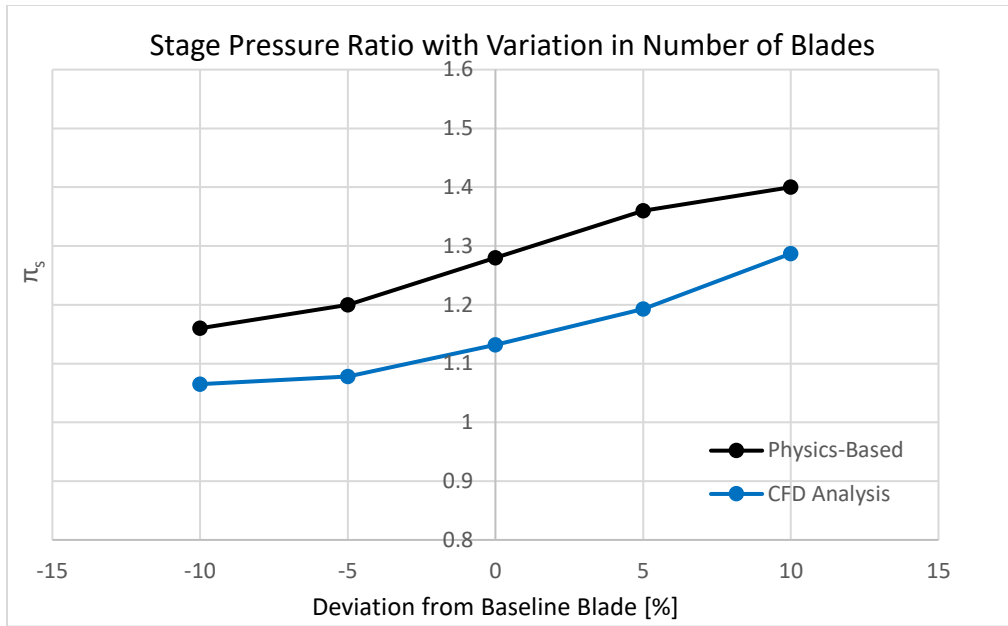


Figure 18. A plot of the stage pressure ratio with variations in the number of blades of the first stage of HPC

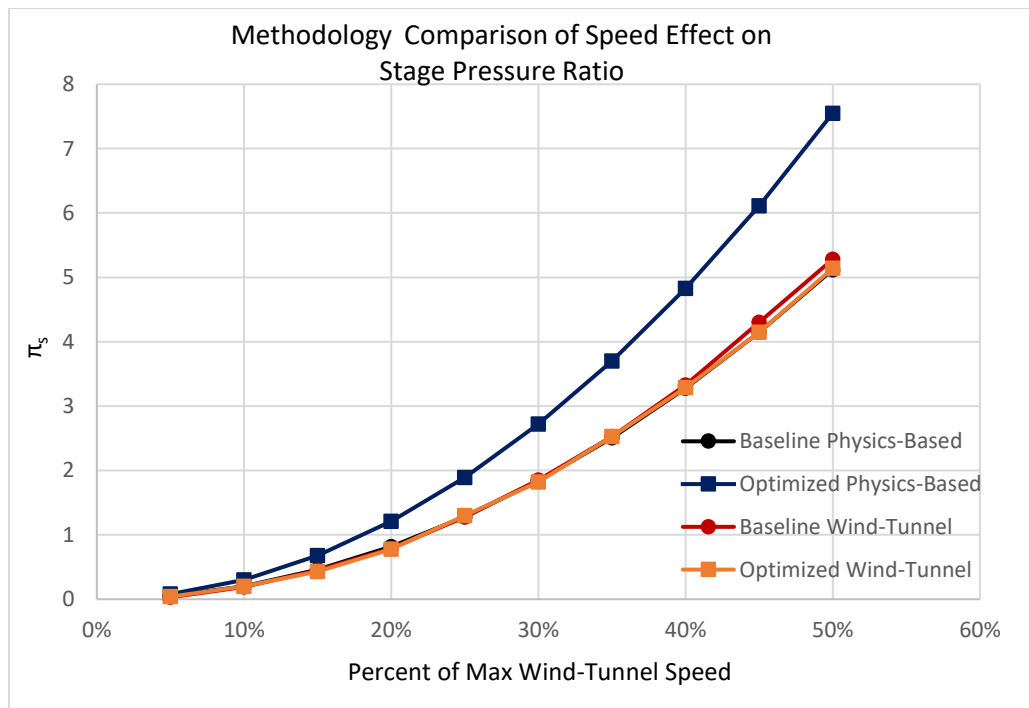


Figure 19. A plot comparing the baseline and optimized stage pressure values with respect to wind-tunnel speed and methodology

Figure 19 compares the results of physics-based modeling and CFD analysis. All four lines display a similar trend of increasing stage pressure ratio as percentage of max speed increases. The baseline physics-based line is difficult to see as it is underneath the wind-tunnel lines. The values for stage pressure ratio are very close to each other for both baseline models for each method. The optimized model from physics-based testing has higher values overall. This can be attributed to the physics-based model relying on ideal conditions. These ideal conditions include no losses due to friction. It can be observed that physics-based modeling will overpredict when compared to the real-wind-tunnel.

VI. CONCLUSIONS

The goal of this research is to optimize the blades of the high-pressure compressor by altering the blade design variables of the rotor blades of the first stage. Using physics-based modeling, CFD analysis, and wind-tunnel testing, it can be concluded that increasing the span, angle of incidence, taper ratio, and number of blades will increase the compressor pressure ratio. In addition, decreasing the twist will also increase the compressor pressure ratio. These results are confirmed by physics-based modeling and CFD analysis. Due to differing results in the chord design variable, more testing and literature review needs to be conducted to determine the actual effect on the compressor pressure ratio the blade chord length has. Wind-tunnel testing shows a trend in increasing stage pressure ratio when increasing the speed of the wind-tunnel. It is also determined that the optimized model does not give higher values of stage pressure ratio. This can lead to the conclusion that a single design variable may have a greater impact on the stage pressure ratio than all the optimized design variables combined.

VII. FUTURE WORK

For future work, additional wind-tunnel testing should be performed on each individual design variable to determine if a single design variable has a greater impact on the stage pressure ratio compared to that of a combination of them. In addition, improvements to the 3D-printed models should be made to ensure proper rotation of the blades to replicate a real high-pressure compressor stage more accurately.

VIII. REFERENCES

- [1] P. Klisz, "Free CAD designs, files & 3D models: The GrabCAD Community Library," *Stratasys Inc.*, Dec. 5, 2016. <https://grabcad.com/library/genx-1b-modified-v-1-0-1>.
- [2] General Electric Company, U.S. Department of Transportation, and Federal Aviation Administration, "Type certificate data sheet E00078NE," no. 3, Apr. 2011. <http://large.stanford.edu/courses/2016/ph240/ginsberg2/docs/E00078NERev3.pdf>
- [3] J. D. Mattingly, *Elements of Gas Turbine Propulsion*. New York: McGraw Hill Inc., 1985, pp. 2-5, 12-20, 299-316, 355-364, 811.
- [4] A. F. El-Sayed, M. S. Emeara, and M. K. Fayed, "Performance analysis of cold sections of high BYPASS ratio turbofan aeroengine," *J. Robot Mech Eng. Research*, vol. 2, no. 1, pp. 18-27, Oct. 2017.
- [5] S. F. Clark, "787 propulsion system," *Boeing*, Mar. 2012. https://www.boeing.com/commercial/aeromagazine/articles/2012_q3/2/